

Optimization of a Digital Controller and Observer in a Two-Mass System - the LQ Problem

Streszczenie: Artykuł przedstawia propozycję sterowania 2-masowym układem napędowym (z połączeniem sprężystym). Przedstawiono system regulacji bazujący na obserwowanych zmiennych stanu: prędkości agregatu i momentu skręcającego. W celu spełnienia ograniczeń prądowych silnika zastosowano dodatkowy regulator PI prądu twornika. Optymalizację regulatora stabilizującego i obserwatora zmiennych stanu przeprowadzono w oparciu o dyskretny problem LQ. W części opisującej badania symulacyjne przedstawiono pracę układu z uwzględnieniem różnych rozdzielcości modelowanych przetworników analogowo-cyfrowych, cyfrowo analogowych oraz długości przetwarzanego słowa procesora (regulacja cyfrowa). (**Optymalizacja cyfrowego regulatora i obserwatora w układzie 2-masowym. Problem LQ.**)

Abstract: The paper describes a proposed control system for a 2-mass electric drive with flexible shaft. The control system utilizes observed state variables: the drive system speed and tensional moment. To meet the motor current limits an additional armature current PI controller is used. Optimization of the stabilizing controller and the state variables observer is based on the discrete-time LQ problem. Further, simulations of the system operation for different resolutions of modelled A/D and DA converters and the processor word lengths (digital control) are described..

Słowa kluczowe: Napęd prądu stałego, układ 2-masowy, połączenie sprężyste, obserwator zmiennych stanu, dyskretny problem LQ, regulacja cyfrowa.

Keywords: DC drive, 2-mass system, flexible shaft, state variable observer, discrete time LQ problem, digital control.

Introduction

The approach to modelling 2-mass systems is related to the type of electric drive used. In economic terms electric drives utilizing AC motors supplied from frequency converters are increasingly popular compared to DC motors. A large number of DC drives with separately excited motors being still operated by industry, is the reason for various modernizations to improve their performance indices. Their unquestionable advantages are good control properties. Seeking for more advanced DC drives control methods is therefore advisable. Another motivating reason for designing DC drives control systems is application of the obtained results to field oriented control (FOC) of AC motors. Furthermore, comparing mathematical models of these two types of drives, i.e. a DC separately excited motor and an induction squirrel cage motor supplied from an inverter with forced current in field oriented coordinates (mathematical model in (d,q) coordinates), it should be noted that the mechanical equation in both drives models is identical:

$$(1) \quad J \frac{d\omega(t)}{dt} = M_e(t) - M_o(t)$$

and they differ solely in the way the electromagnetic torque M_e is produced. This creates an additional possibility for the use of identical load torque observers in both types of drive [15].

The control system structure of 2-mass system with a separately excited DC motor has already been utilized in former publications [16,25] – figure 1.

The control system is comprised of: a 2-mass system, an observer and the current and speed controller. The aim of this investigation is modelling of fixed-point processing phenomena, so as to obtain the control system that satisfies optimum tracking and stabilization of angular velocity.

The paper deals with the observer parameters and controller gain matrix optimization employing the discrete-time linear quadratic problem.

This approach distinguishes the discussed topic from the formerly described problems [16,25]. Additionally, the control system modelling was carried out using the MATLAB-SIMULINK FIXED POINT TOOLBOX library. This allows determining the influence of converters quantization step

and the processor computational accuracy on the control quality and precision.

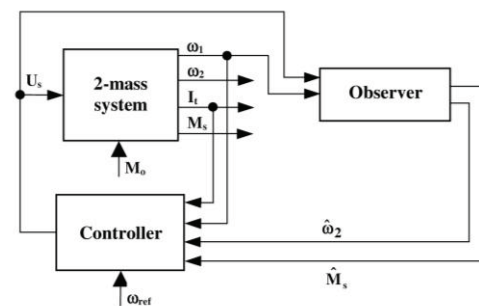


Fig.1. The control system structure of a 2-mass system

The mathematical model of the 2-mass system with flexible coupling

Mathematical description of the 2-mass system is based on a model of an inertia-less elastic element being a compromise between the description complexity and accuracy [5,9,13,16,18,19,20,24,25,27].

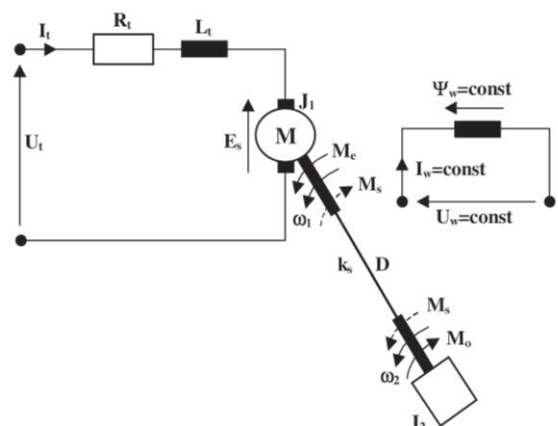


Fig.2. The physical model of a 2-mass system

It is represented by the following set of differential equations:

$$\begin{aligned} U_t(t) &= I_t(t)R_t + L_t \frac{dI_t(t)}{dt} + \psi_e \omega_1(t) \\ J_1 \frac{d\omega_1(t)}{dt} &= (M_e(t) - M_s(t)) - D(\omega_1(t) - \omega_2(t)) \\ (2) \quad J_2 \frac{d\omega_2(t)}{dt} &= (M_s(t) - M_o(t)) + D(\omega_1(t) - \omega_2(t)) \\ \frac{dM_s(t)}{dt} &= k_s(\omega_1(t) - \omega_2(t)) \\ \Delta\varphi(t) &= \varphi_1(t) - \varphi_2(t) = \int_0^t (\omega_1(t) - \omega_2(t)) dt \end{aligned}$$

where: k_s – the shaft modulus of elasticity, D – damping factor of the elastic element oscillations, $M_e(t)$ – electromagnetic torque, $M_o(t)$ – load torque, $M_s(t)$ – torsional moment.

The LQ problem for sampled-data systems

For a linear stationary system described by equation

$$(3) \quad \dot{x}(t) = \tilde{A}x(t) + \tilde{B}u(t)$$

$$x(0) = x_0$$

where: $x \in R^n$, $u \in R^m$,

shall be found the discrete control law (K is the discrete controller gain matrix)

$$(4) \quad u(k) = -Kx(k)$$

minimizing the performance index

$$(5) \quad J_c = \int_0^\infty [x^T(t)\tilde{Q}x(t) + u^T(t)\tilde{R}u(t)] dt$$

where: $\tilde{Q} = Q^T \geq 0$, $\tilde{R} = R^T > 0$.

The LQ problem has a solution if the pair (\tilde{A}, \tilde{B}) is stabilized and the pair (\tilde{Q}, \tilde{A}) is detectable.

There are two methods of solving the LQ problem:

1. Discretization of the equation (3) and performance index (5), then determining the matrix K using discrete algebraic Riccati equation (ARE). This method can be used to determine the control $u(k)$.
2. Discretization of the equation (3) taking the performance index in the discrete form

$$(6) \quad J_1 = \sum_{k=0}^{\infty} [x^T(k)Qx(k) + u^T(k)Ru(k)]$$

then the subsequent computations are carried out analogically as in the method 1. This procedure can be used for both the observer and controller optimization.

Regrettably, the performance of the system designed this way is best during stabilization at the operating point $x=0$. The LQ problem practical applications to control problems are possible if the optimized system is supplemented with an integrator (Fig.1). The integrator is connected with the system main input – for electric drive it is the speed or position.

In order to apply standard algorithms for the LQ problem solving the integrator transmittance

$$G_I(s) = \frac{\rho(s)}{y(s)} = \frac{1}{s}$$

is rewritten in the form of a differential equation

$$\dot{\rho}(t) = y(t)$$

where y is the main state variable – the system output. The equation (3) is subsequently supplemented with the integrator, yielding the extended equation of state:

$$(7) \quad \begin{bmatrix} \dot{x}(t) \\ \dot{\rho}(t) \end{bmatrix} = \begin{bmatrix} \tilde{A} & 0 \\ C & 0 \end{bmatrix} \begin{bmatrix} x(t) \\ \rho(t) \end{bmatrix} + \begin{bmatrix} \tilde{B} \\ 0 \end{bmatrix} u(t)$$

The LQ problem is solved for the extended system (7) yielding the controller gain matrix

$$K = [k_1 \dots k_n \ k_{n+1}]$$

where k_{n+1} is the integrator gain.

The control system structure and optimization

The proposed 2-mass system control structure shown in figure 3 incorporates: the armature current secondary controller and the primary speed controller with stabilizing feedback loop comprising the LQ state controller.

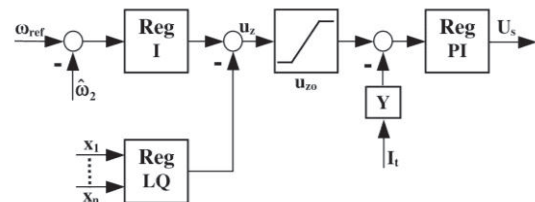


Fig.3. The 2-mass system control structure

The speed controller structure utilizes the LQ optimization based on the model represented by the linear state equation (3). This model is encompassed by feedback loops from all state variables. The controller structure requires the knowledge of all state variables and, consequently, the use of measuring transducers or, where state variable is inaccessible for measuring, a signal reconstruction circuit.

The control equation for the system with the state controller is written in the form of

$$(8) \quad u(t) = -Kx(t)$$

where the state controller

$$(9) \quad K = [k_1 \ k_2 \ \dots \ k_m], \quad x(t) = \begin{bmatrix} x_1(t) \\ x_2(t) \\ \vdots \\ x_n(t) \end{bmatrix},$$

$n=m$, $x(t)$ – the state vector.

The state controller gain coefficients are determined according to the LQ optimization based on minimization of the performance index expressed in the integral form (5). The LQ control ensures very high robustness [1] for the case of the performance index R diagonal matrix. The controller provides gain margin $(\frac{1}{2}, \infty)$ and phase margin 60° .

For these reasons the LQ control is a good solution for systems where the key task is the system state stabilization at the origin of the coordinate system $x(t)=[0 \ 0 \ \dots \ 0]^T$. Unfortunately, adding a summing node results in the occurrence of the proportional feedback loop characteristic feature – the steady-state error. If the control system is intended to stabilize the drive system at various operating points the use of an integral controller is required. This way the proportional-integral LQ control is created.

In order to determine the controller gain matrix we shall pose and solve the infinite horizon time-discrete LQ problem.

Practical realization of the proportional-integral LQ control in a 2-mass system is not possible without optimizing the current (torque) transient shape within the given limitations of its magnitude. The motor starting, loading with torque, as well as failure conditions in the DC circuit must not result in exceeding the motor ratings. It is therefore necessary to implement a current controller that allows for the best utilization of the motor performance ensuring the set current response to the unit step. It is an exponential time curve with the steady state value resulting from the motor permissible current and its maximum time derivative.

$$(10) \quad \left| \frac{dI}{dt} \right| \leq p I_N, \quad |I| \leq \lambda_N I_N$$

where: λ_N and p are the permissible multiplicities of the current and its derivative.

The current controller should be therefore assumed a proportional-integral element whose parameters can be selected employing the shape criterion [5,6]. The effect of mechanical time-constant B is taken into account in this method using the current transfer function

$$(11) \quad G_{2I}(s) = \frac{1}{R_t} \frac{Bs}{BT_t s^2 + Bs + 1}$$

$$\text{where: } B = J \frac{R}{\psi_e^2}, \quad T_t = \frac{L}{R}$$

The thyristor converter is approximated by a proportional element with constant gain coefficient K_p . The current controller $G_{RI}(s)$ parameters: m and V should be determined using the control system block diagram representation as shown in figure 4.

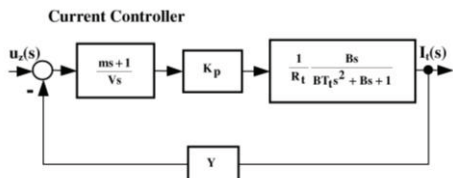


Fig.4. The control system block diagram

Further proceeding is conditioned by the relation between the drive mechanical time constant B and electrical time constant T_t . For electric drives with $B > 4T_t$ (this applies to the investigated system) the transfer function $G_{2I}(s)$ can be written in the form of

$$(12) \quad G_{2I}(s) = \frac{1}{R_t} \frac{Bs}{(B_I s + 1)(T_I s + 1)}$$

where

$$(13) \quad B_I T_I = B T_t \quad \text{i} \quad B_I + T_I = B$$

The above conditions can be satisfied for

$$(14) \quad T_I = 0.5B \left(1 - \sqrt{1 - 4 \frac{T_t}{B}} \right)$$

An element with the following transmittance is taken as the reference model

$$(15) \quad G_z(s) = \frac{k_z}{\beta s + 1}$$

and compared with the closed-loop system transmittance (Fig.5). Thus, we obtain

$$(16) \quad m = T_I, \quad V = \beta \frac{YK_p B}{(B_I - \beta) R_t}$$

where

$$(17) \quad \beta = \frac{\lambda_N}{p} = \frac{VR_t}{VR_t + YK_p B} B_I$$

and the controller input signal limitation ($I_{um} = \lambda_N I_N$)

$$(18) \quad u_{z0} = I_{um} \frac{YB_I}{(B_I - \beta)}$$

Finally, the equivalent coefficient k_z is

$$(19) \quad k_z = \frac{B_I - \beta}{YB_I}$$

The last step is of the current controller $G_{RI}(s)$ discretization [14,26].

Prior to solving the LQ problem, has been determined the drive model in which equations (2) were supplemented with the current controller $G_{RI}(s)$. Therefore the motor voltage equation reduces to the form (15). In order to incorporate the integrator into the control system, the equations of state were complemented according to the relation (7). Consequently, we obtain:

$$x(t) = \begin{bmatrix} \omega_1(t) \\ \omega_2(t) \\ I_t(t) \\ M_s(t) \\ \varphi_2(t) \end{bmatrix}, \quad y(t) = \omega_2(t), \quad u(t) = U_s(t)$$

(20)

$$\tilde{A} = \begin{bmatrix} -\frac{D}{J_1} & \frac{D}{J_1} & \frac{\Psi_e}{J_1} & -\frac{I}{J_1} & 0 \\ \frac{D}{J_2} & -\frac{D}{J_2} & 0 & \frac{I}{J_2} & 0 \\ 0 & 0 & -\frac{I}{\beta} & 0 & 0 \\ k_s & -k_s & 0 & 0 & 0 \\ 0 & 1 & 0 & 0 & 0 \end{bmatrix}, \quad \tilde{B} = \begin{bmatrix} 0 \\ 0 \\ \frac{k_z}{\beta} \\ 0 \\ 0 \end{bmatrix}$$

$$\tilde{C} = [0 \ 1 \ 0 \ 0 \ 0]$$

where: $\dot{\varphi}_2 = \omega_2$, and the performance index (5) is written as follows

$$(21) \quad J_c = \int_0^\infty [x^T(t)Qx(t) + u^T(t)Ru(t) + \varphi_2^T(t)Q_\varphi\varphi_2(t)]dt \\ = \int_0^\infty \begin{bmatrix} x^T(t) & \varphi_2^T(t) \end{bmatrix} \underbrace{\begin{bmatrix} Q & 0 \\ 0 & Q_\varphi \end{bmatrix}}_{Q_r} \begin{bmatrix} x(t) \\ \varphi_2(t) \end{bmatrix} + u^T(t)Ru(t) dt$$

Having given the matrices \tilde{A}, \tilde{B} (20) and selecting Q_r, Q_φ, R , we obtain the state controller K in the MATLAB-SIMULINK environment using the function *lqr*

$$(22) \quad [K, s, e] = lqr(A_t, B_t, Q_r, R, T_s)$$

where

$$(23) \quad K = [k_1 \ k_2 \ k_3 \ k_4 \ k_5]$$

The load torque M_o has been disregarded in the mathematical description (20). It has been considered a disturbance signal, while the proportional-integral LQ control task is to stabilize the drive system at the operating point. It is therefore reasonable that the disturbance matrix and the load-torque signal have been omitted in the mathematical model. This form of the mathematical model is used solely for the control system synthesis purpose, whereas in the simulations the complete mathematical model is employed.

The observer structure

In practical applications the observer operates in a closed feedback loop. In order to overcome difficulties in satisfying the condition $\hat{x}(k) = x(k)$ we propose the use of the error vector $x(k) - \hat{x}(k)$ to improve the observer performance. A lack of knowledge of $x(k)$ can be avoided utilizing the system outputs vector $y(k) = Cx(k)$, thus the error signal is

$$(24) \quad e(k) = y(k) - C\hat{x}(k) = C(x(k) - \hat{x}(k))$$

It should be borne in mind that the error signal (24) can equal zero if $\hat{x}(k) \neq x(k)$. Such situation occurs when the vector $e(k)$ is orthogonal to the matrix C rows. Nevertheless, this is the only way for determining the feedback signal. The estimation error $e(k)$ can be amplified using the matrix L . Thereby the signal of model errors correlation is obtained. This approach allows constructing the observer in a closed feedback loop.

The selection of the observer matrix L begins from defining the error signal (24) and assumption that $e(0) \neq 0$. For an element described with the discrete linear time-invariant state equation is

$$(25) \quad \begin{aligned} x(k+1) &= Ax(k) + Bu(k) \\ y(k) &= Cx(k) \\ x(0) &= x_0 \end{aligned}$$

$$x(k) \in R^n, u(k) \in R^m, y(k) \in R^r$$

and the observer equation is written as

$$(26) \quad \hat{x}(k+1) = A\hat{x}(k) + Bu(k) + LC(x(k) - \hat{x}(k))$$

where: $LC(x(k) - \hat{x}(k))$ is the model errors correction.

For the purposes of a computer system it is convenient to convert the foregoing equation to the form

$$(27) \quad \hat{x}(k+1) = (A - LC)\hat{x}(k) + Bu(k) + Ly(k)$$

For the observer structure determined as above should be selected the error correction matrix. If the observer is determined using a dual system [10,15] in the form of

$$\tilde{x}(k+1) = A^T\tilde{x}(k) + C^T\tilde{u}(k)$$

$$\tilde{y}(k) = B^T\tilde{x}(k)$$

$$(28) \quad \tilde{x}(0) = \tilde{x}_0$$

$$\tilde{x}(k) \in R^n, \tilde{u}(k) \in R^r, \tilde{y}(k) \in R^m$$

resulting in a steady-state feedback with the gain matrix K , then the error correction matrix L is determined from the relation

$$(29) \quad L = K^T$$

Selection of the matrix L is made using the infinite horizon time-discrete LQ problem.

Optimizing the observer

The mathematical model of a 2-mass system can be written in the form of the equation of state

$$(30) \quad \dot{x}(t) = \tilde{A}x(t) + \tilde{B}u(t)$$

$$y(t) = \tilde{C}x(t)$$

where

$$x(t) = \begin{bmatrix} \omega_1(t) \\ \omega_2(t) \\ I_1(t) \\ M_s(t) \end{bmatrix}, \quad y(t) = \omega_1(t), \quad u(t) = U_s(t)$$

and the matrices take the form

$$(31) \quad \tilde{A} = \begin{bmatrix} -D & D & \Psi_e & -I \\ \frac{J_1}{D} & \frac{J_1}{D} & \frac{J_1}{J_1} & \frac{J_1}{J_1} \\ \frac{D}{J_2} & -\frac{D}{J_2} & 0 & \frac{1}{J_2} \\ \frac{J_2}{-\Psi_e} & 0 & -1 & 0 \\ \frac{L}{k_s} & -k_s & 0 & 0 \end{bmatrix}, \quad \tilde{B} = \begin{bmatrix} 0 \\ 0 \\ \frac{K_p}{L} \\ 0 \end{bmatrix}, \quad \tilde{C} = [1 \ 0 \ 0 \ 0]$$

The system discrete form (30) in the MATLAB-SIMULINK environment is obtained using the function *c2d*

$$(32) \quad [A, B] = c2d(A_t, B_t, T_s)$$

$$(33) \quad C = [1 \ 0 \ 0 \ 0]$$

and the error correction matrix L is determined only for the discrete dual system and the performance index (6), using the function *dlqr*

$$(34) \quad [L, s, e] = dlqr(A', C', Q_o, R)$$

where

$$(35) \quad L = [l_1 \ l_2 \ l_3 \ l_4]^T$$

For the computed matrices A, B, C, L the discrete state-observer can be written in the form of (27). The input variables for that way constructed observer are: the motor speed ω_1 and control voltage U_s , while the estimated variables are: the torsional moment \hat{M}_s and the driven machine speed $\hat{\omega}_2$.

Modelling the measuring circuits

Signal processing circuit - from actual analogue signals to digital ones - is a consequence of the fixed-point modeling of both the observer and the (speed and current) controller structures. The key analogue signals are: the motor speed ω_1 and current I_t . The motor speed is an input signal for both the observer and the speed controller. In real systems it can be acquired by means of a tachogenerator or an encoder. The current and speed controller input signal is the motor current. It normally is obtained by means of current transformers or LEM current transducers. The principles of the measuring transducers design and selection of the speed (k_v) or current (Y) feedback are discussed in [5].

The signal processing circuit designed for the purposes of fixed-point modeling is shown in figure 5.

The processed analogue signals should be prepared to conversion into the fixed-point mode. For this purpose are used matching circuits that transform the analogue signal magnitude to a range of decimal numbers from the interval

$$(36) \quad -I \leq X_{(10)} \leq I - \frac{I}{2^{n-1}}$$

where n : n -bit digital information vectors.

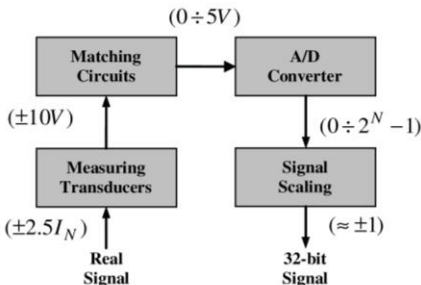


Fig.5. The example of the armature current I_t signal processing circuit (typical ranges of processed signal are given in parenthesis)

In a microprocessor system they correspond to binary numbers in the two's-complement code.

The prepared analogue signals are converted to digital form by means of A/D converters of with a specified, e.g. 10-, 12- or 16-bit resolution. The observer and the controller are designed in a 32-bit fixed-point numbers technique. It is important to trace the decimal point position during fixed-point arithmetic operations and ensure its position is fixed. Therefore the numbers should be scaled.

The simulations research

Simulations were carried out for the structure shown in figure 1 employing the MATLAB-SIMULINK simulation package. The control system (LQ speed controller and PI current controller) and the observer (of torsional moment and the driven machine speed $\hat{\omega}_2$) was realized using 32-bit fixed-point blocks. In order to find differences resulting from the converters resolution, A/D and D/A conversion

was realized using 10-bit, and subsequently 16-bit blocks.

Simulations were carried out for two cases of mass distribution: $J_1 > J_2$ and $J_1 < J_2$.

The drive parameters are contained in the Annex. The simulation includes the drive start-up to the speed of 160[rad/s] and step load with nominal torque M_N . The following signal limitations were applied: the reference voltage u_z was limited to $\pm u_{z0}$, the static converter output voltage U_s was limited within $\pm 10V$.

The selected control circuit parameters for $J_1 > J_2$, and 10-bit and 16-bit A/D and D/A converters are tabulated in table 1 (the controller (23) and observer (35)).

Table 1. Summary of coefficients for the $J_1 > J_2$ case

$J_1 > J_2$	K_1	K_2	K_3	K_4	K_5
	143.42	11.82	66.43	-1.19	234.26
Q		$\begin{bmatrix} 39000 & 0 & 0 & 0 \\ 0 & 1 & 0 & 0 \\ 0 & 0 & 8000 & 0 \\ 0 & 0 & 0 & 8 \end{bmatrix}$			
Q_o		100000			
	L_1	L_2	L_3	L_4	
	0.9998	0.0005	-0.0205	0.0099	
Q_o		$\begin{bmatrix} 39000 & 0 & 0 & 0 \\ 0 & 1 & 0 & 0 \\ 0 & 0 & 8000 & 0 \\ 0 & 0 & 0 & 8 \end{bmatrix}$			
R		1			
T_s		$2 \cdot 10^{-4}s$			
K_1		0.024			
Y		0.58			
u_{z0}		$\pm 8 \cdot 10^{-4}V$			

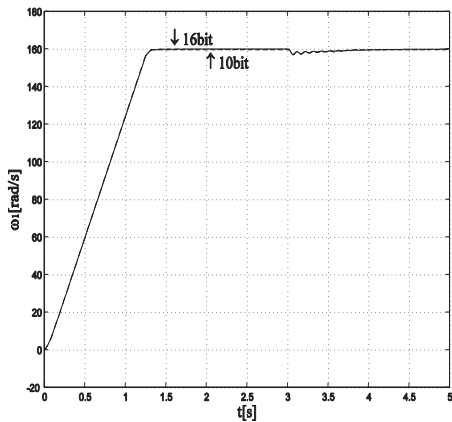


Fig.6. Comparison of the motor speed waveforms for 10-bit and 16-bit A/D and D/A converters for the $J_1 > J_2$ case

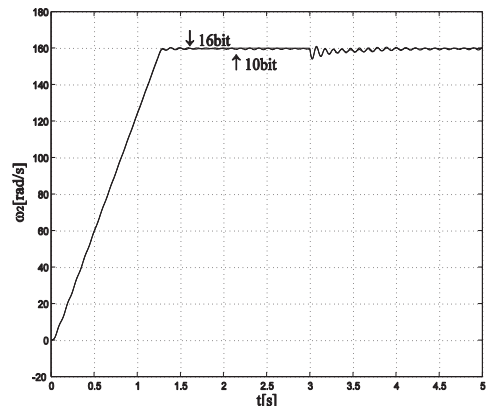


Fig.7. Comparison of the load speed waveforms for 10-bit and 16-bit A/D and D/A converters for the $J_1 > J_2$ case

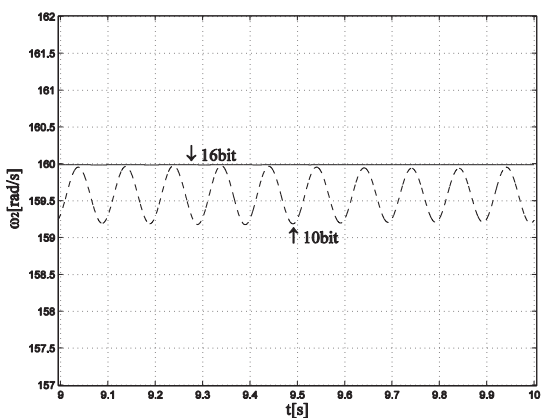


Fig.8. Comparison of the load speed waveforms for 10-bit and 16-bit A/D and D/A converters the $J_1 > J_2$ case – the steady state

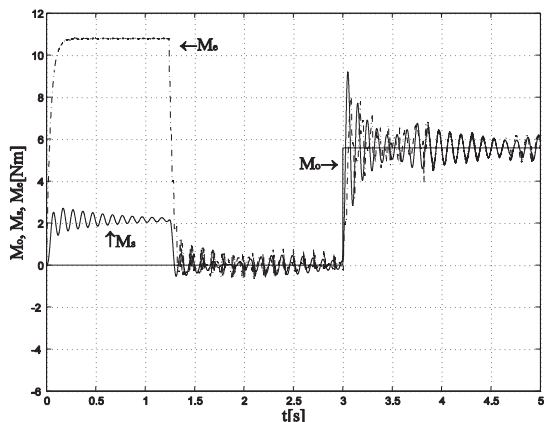


Fig.9. Comparison of the electromagnetic torque and torsional moment waveforms for 10-bit A/D and D/A converters for the $J_1 > J_2$ case

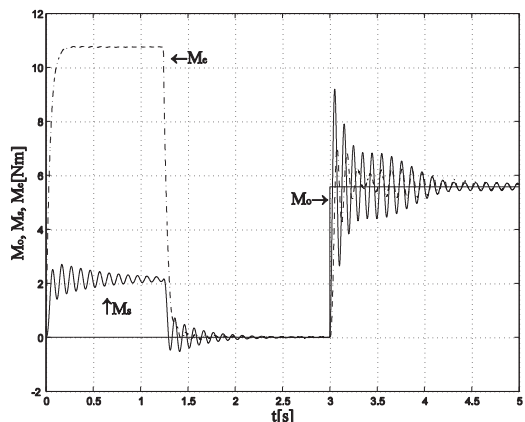


Fig.10. Comparison of the electromagnetic torque and torsional moment waveforms for 16-bit A/D and D/A converters for the $J_1 > J_2$ case

The selected control circuit parameters for $J_1 < J_2$, and 10-bit and 16-bit A/D and D/A converters are tabulated in table 2.

Table 2. Summary of coefficients for the $J_1 < J_2$ case

	K_1	K_2	K_3	K_4	K_5
$J_1 < J_2$	61.07	121.03	77.68	24.64	270.58
Q		$\begin{bmatrix} 250 & 0 & 0 & 0 \\ 0 & 38800 & 0 & 0 \\ 0 & 0 & 8000 & 0 \\ 0 & 0 & 0 & 8 \end{bmatrix}$			

Q_0	100000			
	L_1	L_2	L_3	L_4
	1.06	11.69	0.82	-4.44
Q_0	250	0	0	0
	0	38800	0	0
	0	0	8000	0
	0	0	0	8
R		1		
T_s		$2 \cdot 10^{-4}$ s		
K_t		0.024		
Y		0.58		
u_{z0}		$\pm 9.3 \cdot 10^{-4}$ V		

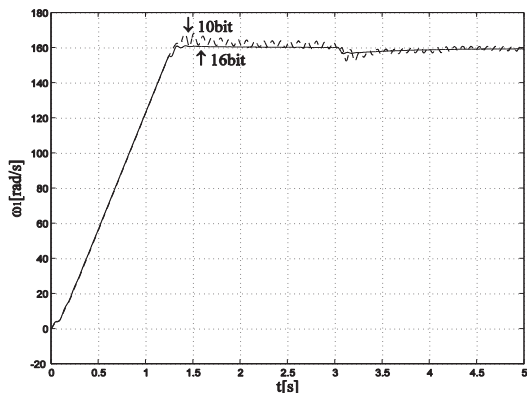


Fig.11. Comparison of the motor speed waveforms for 10-bit and 16-bit A/D and D/A converters for the $J_1 < J_2$ case

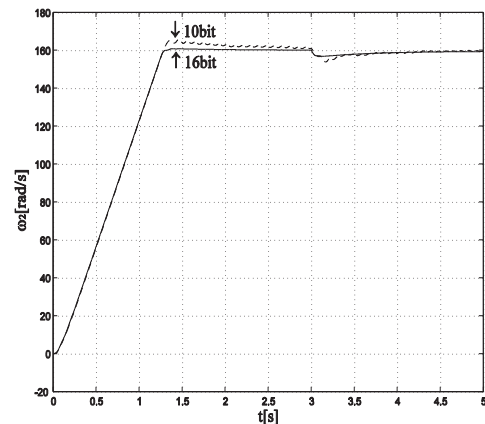


Fig.12. Comparison of the load speed waveforms for 10-bit and 16-bit A/D and D/A converters for the $J_1 < J_2$ case

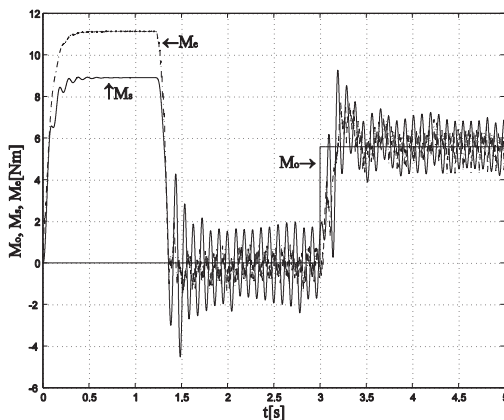


Fig.13. Comparison of the electromagnetic torque and torsional moment waveforms for 10-bit A/D and D/A converters for the $J_1 < J_2$ case

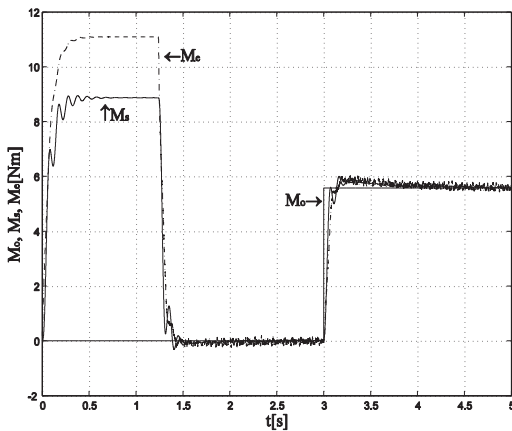


Fig.14. Comparison of the electromagnetic torque and torsional moment waveforms for 16-bit A/D and D/A converters for the $J_1 < J_2$ case

The selected control circuit parameters for $J_1 < J_2$, and 10-bit A/D and D/A converters and the best possible choice of Q_r and Q_o matrices are tabulated in table 3.

Table 3. Summary of coefficients for the $J_1 < J_2$ case (the performance index coefficients are different from those in table 2)

	K ₁	K ₂	K ₃	K ₄	K ₅
$J_1 < J_2$	93.5	91.56	78.81	26.11	269.93
Q		$\begin{bmatrix} 6800 & 0 & 0 & 0 \\ 0 & 33800 & 0 & 0 \\ 0 & 0 & 8000 & 0 \\ 0 & 0 & 0 & 8 \end{bmatrix}$			
Q_o		100000			
	L ₁	L ₂	L ₃	L ₄	
	1.04	5.42	0.24	-2.98	
Q_o		$\begin{bmatrix} 1000 & 0 & 0 & 0 \\ 0 & 33800 & 0 & 0 \\ 0 & 0 & 8000 & 0 \\ 0 & 0 & 0 & 8 \end{bmatrix}$			
R		1			
T _s		$2 \cdot 10^{-4}$ s			
K _t		0.024			
Y		0.58			
u _{z0}		$\pm 9.3 \cdot 10^{-4}$ V			

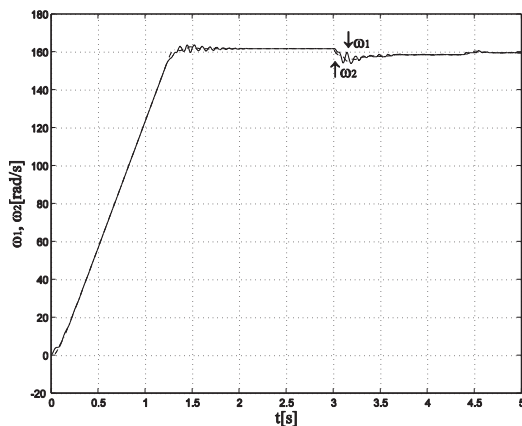


Fig.15. The motor and the load speed waveforms for 10-bit A/D and D/A converters and the best possible choice of Q_r and Q_o matrices for the $J_1 < J_2$ case

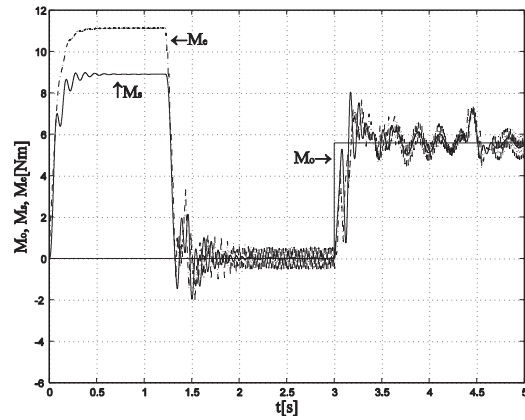


Fig.16. The electromagnetic torque and torsional moment waveforms for 10-bit A/D and D/A converters and the best possible choice of Q_r and Q_o matrices for the $J_1 < J_2$ case

Conclusion

The digital control of the 2-mass drive system with a separately excited motor is presented in the paper. The time-discrete LQ problem is employed in design of the speed controller and the state variables observer. The choice of the performance index weight coefficients matrices is provided. Furthermore, the measurement results are compared taking into account the selectivity of applied 10-bit and 16-bit A/D (D/A) converters. The system transient behaviour becomes less oscillatory with the increase in both: the moment of inertia and the A/D (D/A) converters resolution. Thus the best possible choice of the matrices Q_r and Q_o was made, so that using 10-bit A/D (D/A) converters the investigated waveforms quality was as close as possible to those recorded with 16-bit converters. The presented system shows good stabilizing properties. In the case of $J_1 < J_2$ and 16-bit converters the driven machine speed ω_2 drop under nominal torque step load was ca. 2% whereas for 10-bit converters it was ca. 3.2%.

The dynamic error for $J_1 > J_2$ and 16-bit converters was 3.67%, whereas for 10-bit converters it was 3.78%.

Nonlinearities associated with the fixed-point signal conversion (the effects A/D converters quantization and fixed-point processor) are most evident in the cases illustrated in figures 11 and 12.

The steady-state error and limit cycle achieved in the simulation with 10-bit converters are shown in figure 8. These results suggest that in a real system only small oscillations may occur in steady state.

Appendix

Motor

$$P=1[\text{kW}] \quad U_t=220[\text{V}] \quad I_t=5.75[\text{A}] \quad U_w=220[\text{V}] \quad I_w=0.9[\text{A}] \quad R_t=4[\Omega]$$

$$L_t=0.008[\text{H}] \quad n=2000 \left[\frac{\text{obr}}{\text{min}} \right] \quad \lambda=2 \left[\frac{I_{\max}}{I_t} \right] \quad p=50I_t \left[\frac{\text{A}}{\text{s}} \right]$$

$$K_p=51.3 \left[\frac{\text{V}}{\text{V}} \right] \quad \psi_c=0.97 \left[\frac{\text{Vs}}{\text{rad}} \right], \left[\frac{\text{Nm}}{\text{A}} \right] \quad J_1 = \begin{cases} 0.0167 \left[\frac{\text{kgm}^2}{\text{kg}} \right] \\ 0.0667 \left[\frac{\text{kgm}^2}{\text{kg}} \right] \end{cases}$$

Flexible coupling (shaft)

$$D=0.04 \left[\frac{\text{Nms}}{\text{rad}} \right] \quad k_s=53 \left[\frac{\text{Nm}}{\text{rad}} \right]$$

The load moments of inertia

$$J_2 = \begin{cases} 0.0167 \text{ [kgm}^2] \\ 0.0667 \text{ [kgm}^2] \end{cases}$$

REFERENCES

- [1] Anderson B. D. O., Moore J. B., *Optimal control: Linear Quadratic methods*, Prentice Hall, NJ, (1990)
- [2] Astrom K., Wittenmark B., *Computer-Controlled systems*, NJ, Prentice Hall (1997)
- [3] Callier F. M., Desoer C. A., *Linear System Theory*. New York, Springer-Verlag (1991)
- [4] Chen T., Francis B., *Optimal Sampled-Data Control Systems*, Springer-Verlag (1995)
- [5] Ciepiela A., *Automatic Control of Converter-Fed DC Drives*, Kraków, Wydawnictwa AGH (1992) (in polish)
- [6] Ciepiela A., *Automatic Control of Leonard System*, Kraków, Wydawnictwa AGH (1994) (in polish)
- [7] Dorato P., Abdullah C., Cerone V., *Linear-Quadratic Control: An Introduction*, Prentice Hall, NJ (1995)
- [8] Dorato P., Levis A. H., Optimal Linear Regulators: The discrete-Time Case, *IEEE Tran. on Aut. Cont.* 16 (1972), nr 6, 613-620
- [9] Gierlotka K., *Control Systems of the drives with elastic joint*, Gliwice, Zeszyt Naukowy Politechniki Śląskiej, Nr 1181, (1992) (in polish)
- [10] Kwakernaak H., Sivan R., *Linear Optimal Control Systems*, New York, Wiley Interscience (1972)
- [11] Levis A., Schlueter R., Athans M., On the behaviour of optimal linear sampled-data regulators, *Int. J. Control.* 13, (1971), nr 2, 343-361
- [12] Mitkowski W., *Dynamical System stabilization*, Warszawa, WNT (1991) (in polish)
- [13] Mysiński W., *Microprocessor Control of the Drive with Elastic Joint*, Kraków, AGH (1998) (PhD Thesis)
- [14] Ogata K., *Discrete-Time Control Systems*, Prentice Hall, NJ, (1995)
- [15] Sieklucki G., Orzechowski T., Tondos M., Sykulski R., Optimization of load torque observer at quadratic performance index, *Przegląd Elektrotechniczny*, 84 (2008), nr7, 29-35
- [16] Sieklucki G., Tondos M., Pracownik A., Variable structure control method of a two-mass drive system, *Elektrotechnika i Elektronika*, Wyd. AGH, 26 (2007), 1-2, 69-78
- [17] Sima V., *Algorithms for Linear-Quadratic Optimalization*, Marcel Dekker, Inc. (1995)
- [18] Szabat K., *Analysis of the DC Drive Control Systems with Elastic Joint with Classical and Fuzzy Controllers*, Wrocław, Politechnika Wrocławskiego (2003) (PhD Thesis)
- [19] Szklarski L., Dziadecki A., Strycharz J., Jaracz K., *Automatic Control of Electric Drive*, Kraków, Wyd. AGH (1996)
- [20] Szklarski L., Jaracz K., *Selected Problems of DC drives dynamics*, Kraków, Skrypty uczelniane, Wyd. AGH (1981)
- [21] Tondos M., *Load Torque Reconstruction in Metallurgic Drives*, Kraków, Elektrotechnika, ZN AGH, z. 17, (1990)
- [22] Tondos M., Load Torque Reconstruction in Drives with elastic joint, *Seminarium z Podstaw Elektrotechniki i Teorii Obwodów*, SETO, 1992, 309-316
- [23] Tondos M., Minimizing electromechanical oscillations in the drives with resilient couplings by means of state and disturbance observers, *Fifth European Conference on Power Electronics and Applications*, Brighton, EPE (1993), 360-365
- [24] Tondos M., Mysiński W., Microcomputer-based control system for drivers with resilient couplings, *Proc. of EPE'01*, Graz (2001)
- [25] Tondos M., Sieklucki G., Pracownik A., Proportional-Integral LQ Control of a Two-Mass System, *EPE-PEMC06*, Portoroz (2006)
- [26] Vaccaro J.R., *Digital Control. A State-Space Approach*, Mc Graw-Hill, Inc. (1995)
- [27] Zaleśny P., *Drive Control Systems with Elastic Joint of Improved Dynamical Properties*, Gliwice, Politechnika Śląska (1998) (PhD Thesis)

Autorzy: mgr inż. Adam Pracownik, ArcelorMittal ul. Ujastek 1, 30-969 Kraków, E-mail: Adam.Pracownik@arcelormittal.com; dr inż. Grzegorz Sieklucki, dr hab. inż. Maciej Tondos, Akademia Górniczo-Hutnicza Wydział Elektrotechniki, Automatyki, Informatyki i Elektroniki Katedra Automatyki Napędu i Urządzeń Przemysłowych al. Mickiewicza 30 30-059 Kraków
E-mail: sieklo@kaniup.agh.edu.pl
E-mail: tondos@uci.agh.edu.pl